

Set membership parameter estimation in the frequency domain based on complex intervals

Tarek Raïssi ^a, Nacim Ramdani ^b, Yves Candau ^c

^a*IMS, Université de Bordeaux, 351 cours de la Libération, 33405 Talence, France*

^b*INRIA Sophia Antipolis - Méditerranée and LIRMM, CNRS Université Montpellier 2, 161 rue Ada, 34392 Montpellier cedex 5, France*

^c*CERTES, Université Paris XII, 61 Avenue du Général de Gaulle, 94010 Créteil cedex, France*

Abstract

This paper is devoted to set membership parameter estimation for non-linear complex-valued models. In such a context, the error between the measured data and the output model is supposed to be bounded with known prior bounds. The proposed approach is based on set inversion via *complex interval analysis*. A first contribution of this paper is the extension of logarithm and exponential functions to polar intervals. In a second part, it is shown on an engineering application devoted to thermal parameter estimation, that the proposed interval complex representation is useful.

Key words: Parameter estimation, set-membership estimation, complex intervals, complex constraint satisfaction, set inversion.

1 Introduction

In the literature, parameter estimation problems are usually solved by probabilistic methods when an explicit characterization of the errors and the uncertainties are available. In practice, this is not usually the case for many reasons such as the presence of deterministic modelling errors which cannot

* Corresponding author T. Raïssi. Tel. +33.5.40.00.24.13. Fax +33.5.40.00.66.44
Email addresses: Tarek.Raïssi@ims-bordeaux.fr (Tarek Raïssi),
Nacim.Ramdani@lirmm.fr (Nacim Ramdani), Candau@univ-paris12.fr (Yves Candau).

be taken as random variables. It is then more natural to assume that the perturbations belong to a known set but are otherwise unknown. In such a case, bounded-error approaches allow the characterization of the set of all parameter vectors that are compatible with (i) the measured data, (ii) a model structure and (iii) the prior error bounds. The problem of parameter estimation in a bounded error context has been investigated by many researchers and several techniques have been established for characterizing the posterior feasible set (see Milanese et al. (1996) and the references therein). For linear models, simple-shaped forms such as ellipsoids, parallelotopes, zonotopes or boxes are used to give an enclosure of this set (Durieu et al., 2001; Maksarov et al., 2002) whereas for non-linear models, techniques based on interval analysis and constraint satisfaction techniques are used ((Jaulin et al., 1993, 2001) and references therein).

Many real-life engineering problems can be modelled by differential equations which are nonlinear w.r.t physical parameters but linear w.r.t inputs. Set membership estimation can then be tackled in the frequency domain: the system is then described by a complex-valued nonlinear model. In a bounded error context, the uncertainties are thus described by complex sets. As a result, the derivation of an optimal inclusion function for a complex-valued non-linear model is a major issue for ensuring efficiency for the identification procedure. The simplest complex interval approximation is the rectangular representation (Alefeld et al., 1983; Petkovic et al., 1998), where a complex-shaped set is approximated by an axis-aligned rectangle. Nevertheless, the circular form (Alefeld et al., 1983; Petkovic et al., 1998; Henrici, 1971; Klatte et al., 1980; Rokne et al., 1971) is often used. Unfortunately, both complex interval representations cited above derive very pessimistic results with non-linear functions. To reduce such a pessimism, we introduced in a previous paper (Candau et al., 2006) an arithmetic for complex intervals based on the extension of polar representation of complex numbers to intervals. The main advantage of this representation is that the multiplication operation is exactly defined. However, this is no more the case for the addition operation and a new algorithm was developed for this purpose (Candau et al., 2006). In this paper, the main functions such as logarithm and exponential used in the parameter identification section are extended to polar intervals. In the second part, the performances of the new complex interval arithmetic are evaluated in the context of bounded error identification of thermal parameters.

The paper is structured as follows: in section 2, set membership identification is recalled. The section 3 is devoted to complex interval arithmetics and the extension to polar intervals of non-linear functions such as log, exp, cosh and sinh represents the first contribution of this paper. Section 4 is dedicated to constraint propagation on polar complex intervals. Finally, polar complex intervals are used to solve the parameter estimation problem using actual data and the obtained results are compared to the ones given by the rectangular

complex representation.

2 Set membership identification

Denote by $\mathbf{y}_m(\mathbf{p})$ the model output vector, $\tilde{\mathbf{y}}$ the experimental data vector and \mathbb{E} a feasible domain for the output error, known prior to the identification. The feasible domain for model output is then given by:

$$\mathbb{Y} = \tilde{\mathbf{y}} + \mathbb{E} \quad (1)$$

A parameter vector \mathbf{p} is called *feasible* if the model output is compatible with the measured data domain. Estimating the parameter vector \mathbf{p} in a bounded error context consists in determining the set \mathbb{S} of all feasible parameters:

$$\mathbb{S} = \{\mathbf{p} \in \mathbb{P} \mid \mathbf{y}_m(\mathbf{p}) \in \mathbb{Y}\} = \mathbf{y}_m^{-1}(\mathbb{Y}) \cap \mathbb{P} \quad (2)$$

where \mathbb{P} is a search domain for the parameter vector.

The characterization of the solution set \mathbb{S} is a *set inversion problem* and a guaranteed approximation of such a set can be provided by SIVIA algorithm (Set Inversion Via Interval Analysis) (Jaulin et al., 1993) based on interval analysis. SIVIA is a recursive algorithm which explores all the search space without losing any solution. This algorithm permits to derive a guaranteed enclosure of the solution set \mathbb{S} as follows:

$$\underline{\mathbb{S}} \subseteq \mathbb{S} \subseteq \overline{\mathbb{S}} \quad (3)$$

where $\underline{\mathbb{S}}$ and $\overline{\mathbb{S}}$ are respectively the inner and the outer approximations of \mathbb{S} . The complexity of SIVIA is exponential with respect to the number of parameters and constraint satisfaction techniques are used in order to reduce the computing time.

In this paper, set-membership parameter estimation is performed in the frequency domain using SIVIA and constraint satisfaction techniques. An inclusion test should be defined in order to prove that a parameter set is , unfeasible or undetermined. This test is based on the evaluation of the output model $\mathbf{y}_m(\mathbf{p})$ using complex interval analysis. In the following sections, polar arithmetic is detailed and optimal inclusion functions of the main used functions are proposed.

3 Complex interval analysis

The simplest complex interval representation is the rectangular form where a complicated shaped set is approximated by a rectangle; but the circular form, where a set is approximated by a disc, is more often used. Unfortunately, both complex interval representations cited above are not closed with respect to the arithmetic operations $\{+, -, *, \setminus\}$. This is due to the fact that a multiplication of a set by a complex number is a rotation, thus the result of such an operation must be wrapped in a rectangle or a disc, which introduces some pessimism. The arithmetic operation $*$ is then non minimal and a pessimism is introduced when a multiplication of two complex intervals, represented by rectangles or discs, is performed (Alefeld et al., 1983; Petkovic et al., 1998; Henrici, 1971; Klatte et al., 1980; Rokne et al., 1971; Kearfott, 1996; Nickel, 1980).

In a recent paper (Candau et al., 2006), we extended the polar representation of complex numbers to the case of intervals. It was proved that both the multiplication and the division are exact operations: the result of the multiplication of two polar complex intervals is a polar interval. Nevertheless, this property is not satisfied for addition and subtraction. In (Candau et al., 2006), algorithms are given in order to reduce the pessimism of these operations. In the following, the polar representation is recalled and the extension of the main functions to polar intervals represents the first contribution of this paper.

3.1 Polar representation and arithmetic operations

Consider the intervals $[\rho] = [\rho^-, \rho^+] \in \mathbb{IR}^+$ and $[\theta] = [\theta^-, \theta^+] \in \mathbb{IR}$ where \mathbb{IR}^+ is the set of positive intervals (i.e. $\rho^- \geq 0$). The set defined by:

$$Z = \{z \in \mathbb{C} \mid z = \rho e^{i\theta}, \rho \in [\rho], \theta \in [\theta]\} \quad (4)$$

is called a polar complex interval (or a sector) denoted by

$$Z \triangleq \{[\rho], [\theta]\} \quad (5)$$

A polar interval can be uniquely characterized by two real intervals: its magnitude $[\rho]$, and its angle $[\theta]$ as illustrated in figure 1. The set of all polar complex intervals is denoted by $S(\mathbb{C})$.

To ensure uniqueness of the representation, we can always choose the bounds of the angle interval such that:

$$0 \leq \theta^+ - \theta^- \leq 2\pi, \quad 0 \leq \theta^- < 2\pi, \quad 0 \leq \theta^+ < 4\pi \quad (6)$$

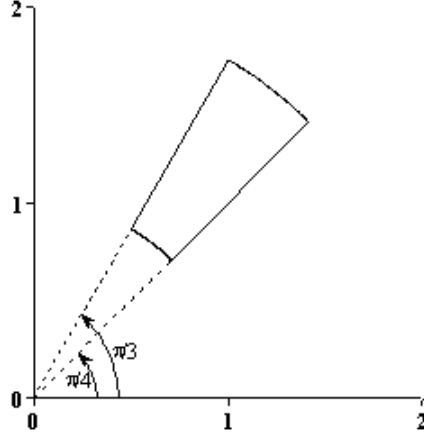


Fig. 1. A sector orientation

Remark: Given $Z = \{[\rho], [\theta]\}$, if $[\rho] = [0, 0]$, then Z is represented by $\{[0, 0], [0, 2\pi]\}$. ■

Let $Z_1 = \{[\rho_1], [\theta_1]\}$ and $Z_2 = \{[\rho_2], [\theta_2]\}$ be two sectors, the multiplication operation between Z_1 and Z_2 is defined as follows:

$$\begin{aligned} Z_1 * Z_2 &= \{z_1 * z_2 \mid z_1 \in [z_1], z_2 \in [z_2]\} \\ &= \{[\rho_1] * [\rho_2], [\theta_1] + [\theta_2]\} \end{aligned} \quad (7)$$

Since the set of real intervals is closed with respect to addition and multiplication, the product of two sectors is also a sector; this operation is then minimal. Similarly, the division is defined by:

$$\left(\begin{aligned} Z_1/Z_2 &= \{z_1/z_2 \mid z_1 \in [z_1], z_2 \in [z_2]\} \\ &= \{[\rho_1]/[\rho_2], [\theta_1] - [\theta_2]\} \end{aligned} \right) \quad (8)$$

where $0 \notin [\rho_2]$. We should note that the argument bounds of the result may not verify (6). In such a case, we add $2k\pi$, $k \in \mathbb{Z}$ to the argument of the computed sector until (6) is met. The following example illustrates this phenomenon.

Example: Given two sectors $Z_1 = \{[1, 2], [2\pi/3, \pi]\}$ and $Z_2 = \{[1, 2], [5\pi/3, 2\pi]\}$. By using expression (7), we have:

$$Z_p = Z_1 * Z_2 = \{[1, 2] * [1, 2], [2\pi/3, \pi] + [5\pi/3, 2\pi]\} = \{[1, 4], [7\pi/3, 3\pi]\}$$

Obviously, the sector Z_p does not respect the condition (6) and -2π is added to its argument. Thus, a sector Z with a same magnitude and with an angle

which respects (6) is obtained. In figure 2, the sectors Z_1 , Z_2 , Z_p and Z are plotted in the (magnitude,angle)-plan. It is easy to note that the sector Z is obtained by a vertical translation of Z_p .

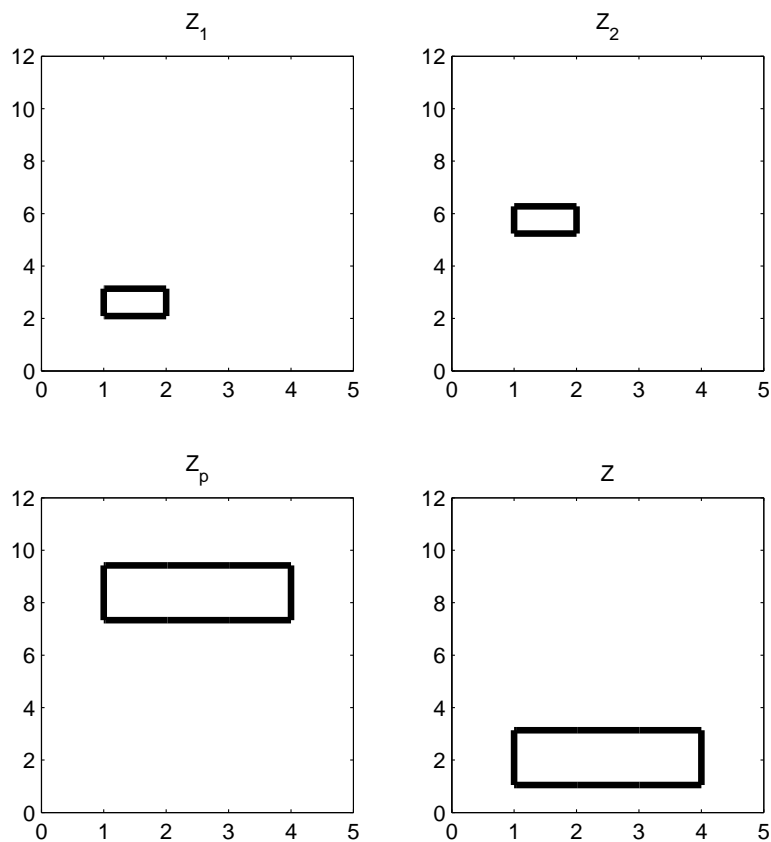


Fig. 2. The product of the sectors Z_1 and Z_2 . Z_p is computed by (7), it does not respect (6). Z is the *true* result which respects (6).

Consider now the addition, the set:

$$Z_1 \oplus Z_2 = \{z_1 + z_2 \mid z_1 \in [z_1], z_2 \in [z_2]\} \quad (9)$$

known as the *Minkowski* sum (Farouki et al., 2002) is not a sector but has a complex shape. To define addition as an operation in $S(\mathbb{C})$, one has to determine some element of $S(\mathbb{C})$ which contains this set. Some degree of pessimism will thus be introduced. To minimize the pessimism, we define $Z_1 + Z_2$ as the smallest sector (see figure 3), in the sense of inclusion, containing $Z_1 \oplus Z_2$:

$$Z_1 + Z_2 = \bigcap Z, \quad Z \in S(\mathbb{C}) \quad (10)$$

$Z_1 + Z_2$ defined in this way exists as an element of $S(\mathbb{C})$, because the intersection of any number of closed boxes is a closed box in \mathbb{R}^2 .

In (Candau et al., 2006), computing the lower and upper bounds of $[\rho]$ and $[\phi]$ is formulated as optimization problems which are solved analytically since the number of variables is only 3. For more details about these algorithms see (Candau et al., 2006).

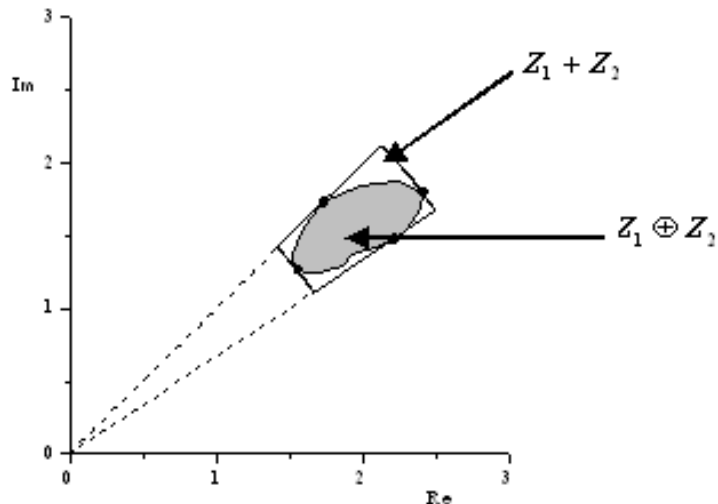


Fig. 3. Minkowski sum - minimal sum of two sectors

Remark: Subtraction is defined in the same way, and does not in fact necessitate a separate treatment from addition, because $Z_1 - Z_2 = Z_1 + (-Z_2)$, where $(-Z_2) = \{z \mid -z \in Z_2\}$.

When physical parameter identification is performed in the frequency domain one usually meets functions such as logarithm, exponential, hyperbolic sine, hyperbolic cosine and their reciprocal functions (acosh, ...). Their extension to polar intervals represents a first contribution of this paper.

3.2 Minimal inclusion function for $\log(Z)$

The aim of this part is to compute the minimal union of sectors containing the range of the function $\log(Z)$ where Z is a sector. Let $\log(r)$ be the natural logarithm of a positive real number r . The logarithm of a non-nul complex number $z = re^{i\theta}$ is defined by:

$$\log(z) = \log(r) + i\theta \quad (11)$$

Hence,

$$\log(z) = \log|z| + i\arg(z), \quad z \neq 0 \quad (12)$$

In (12), the function $\arg(z)$ is an arbitrary determination of the angle of z and the complex number z has an infinite logarithm evaluations with a real part defined in a unique way and an imaginary part containing a 2π additive term. The principal determination of $\log(z)$ is given by:

$$\log(z) = \log|z| + i\text{Arg}(z), \quad z \neq 0, \quad -\pi < \text{Arg}(z) \leq \pi \quad (13)$$

where $\text{Arg}(z)$ is the principal determination of $\arg(z)$. It is trivial to prove that the form (13) is *univaluated*. Nevertheless, the function $\log(z)$ defined by (13) is holomorphic only over the domain $\text{Arg}(z) \in]-\pi, \pi[$. Hence, the negative real half-axis is discarded. In the other hand, inclusion functions do not need holomorphic property, the domain $\text{Arg}(z) \in]-\pi, \pi]$ is then considered.

Consider now a sector $Z = \{[\rho], [\theta]\}$. Since the angle $[\theta]$ of Z has to satisfy the inequalities:

$$0 \leq \theta^+ - \theta^- \leq 2\pi, \quad 0 \leq \theta^- \leq 2\pi, \quad 0 \leq \theta^+ < 4\pi$$

the complex-valued function

$$\log([Z]) = \log([\rho]) + i[\theta] \quad (14)$$

could not be an inclusion function for $\log(z)$. Indeed, in the expression (13) of the \log function, the term $\text{Arg}(z)$ should satisfy the condition : $\text{Arg}(z) \in]-\pi, \pi]$. As the angle of the $\log(Z)$ should verify (6), the main difficulty consists in handling the angles $[\pi, 2\pi]$, $[2\pi, 3\pi]$ and $[3\pi, 4\pi]$. This difficulty is shown in the following example.

Numerical example: The sector $Z = \{[\rho], [\theta]\} = \{[1, 1], [\frac{2\pi}{3}, \frac{4\pi}{3}]\}$ does not respect the condition (6). By using the expression (14), we have:

$$\begin{aligned} \log([\rho]) + i[\theta] &= \log([1, 1]) + i[\frac{2\pi}{3}, \frac{4\pi}{3}] \\ &= \{[\frac{2\pi}{3}, \frac{4\pi}{3}], \frac{\pi}{2}\} \end{aligned} \quad (15)$$

In the other hand, the sector Z can be decomposed in two sectors Z_1 and Z_2 such that:

$$Z = Z_1 \cup Z_2$$

where:

$$\begin{cases} Z_1 = \{[1, 1], [\frac{2\pi}{3}, \pi]\} \\ Z_2 = \{[1, 1], [\pi, \frac{4\pi}{3}]\} \end{cases}$$

The evaluation of the logarithm function over the sector Z_1 is given by:

$$\log(Z_1) = i[\frac{2\pi}{3}, \pi] \equiv \{[\frac{2\pi}{3}, \pi], \frac{\pi}{2}\}$$

In addition

$$\forall z \in Z_2, \quad \log(z) = \log(|z|) + i(\arg(z) - 2\pi)$$

Hence

$$\log(Z_2) = -i[\frac{2\pi}{3}, \pi] \equiv \{[\frac{2\pi}{3}, \pi], \frac{3\pi}{2}\}$$

As $\log(Z_2)$ is not included in $\log(Z)$ computed using (15), the evaluation (14) could not be an inclusion function of $\log(z)$. In the following section, a general method to compute an inclusion function of $\log(z)$ is proposed.

General case:

Consider a sector $Z = \{[\rho], [\theta]\}$ and denote:

$$\begin{cases} Z_1 = \{[\rho], [\theta_1]\} \\ Z_2 = \{[\rho], [\theta_2]\} \\ Z_3 = \{[\rho], [\theta_3]\} \\ Z_4 = \{[\rho], [\theta_4]\} \end{cases} \quad (16)$$

where:

$$\begin{cases} \theta_1 = [\theta] \cap [0, \pi] \\ \theta_2 = [\theta] \cap [\pi, 2\pi] \\ \theta_3 = [\theta] \cap [2\pi, 3\pi] \\ \theta_4 = [\theta] \cap [3\pi, 4\pi] \end{cases} \quad (17)$$

According to (16) and (17), we obtain:

$$\begin{cases} \log(Z_1) = \log([\rho]) + i[\theta_1] & \equiv \{[\rho_1], [\phi_1]\} \\ \log(Z_2) = \log([\rho]) + i([\theta_2] - 2\pi) & \equiv \{[\rho_2], [\phi_2]\} \\ \log(Z_3) = \log([\rho]) + i([\theta_3] - 2\pi) & \equiv \{[\rho_3], [\phi_3]\} \\ \log(Z_4) = \log([\rho]) + i([\theta_4] - 4\pi) & \equiv \{[\rho_4], [\phi_4]\} \end{cases} \quad (18)$$

where ρ_i and ϕ_i are the magnitude and angle of Z_i and with $\log(\{[\rho], \emptyset\}) = \emptyset$. Finally, the inclusion function for logarithm operator is characterized by:

$$\log(Z) = \bigcup_{i=1, \dots, 4} \log(Z_i) \quad (19)$$

We can see that the logarithm of a sector becomes a set of 4 sectors at most, then, computing again the logarithm of the result may lead to 4^2 sectors. Clearly, the evaluation of the inclusion function (19) is combinatorial. Therefore, we suggest to use as inclusion function, the convex hull defined in the following equation

$$\log(Z) = \text{ConvexHull}(\log(Z_i)_{i=1, \dots, 4}) \quad (20)$$

Numerical example: Consider the sector $Z = [\exp(1), \exp(2)], [7\pi/4, 13\pi/4]$. As shown in figure 4, Z must be splitted into 3 sectors Z_1 , Z_2 and Z_3 as explained above. The evaluations of the logarithm function over these sectors are plotted on figure 5. $\log(Z)$ is taken as the convex hull of $\log(Z_i)_{i=1, 2, 3}$.

3.3 Enclosure of $\exp(Z)$

Consider the mapping of a sector by the transformation $z \mapsto \exp(z)$. A complex number $z = \{\rho, \theta\}$ is given in the Cartesian plan by:

$$z = \{\rho, \theta\} = \rho \cos \theta + i\rho \sin \theta$$

According to this consideration, we have :

$$\begin{cases} \exp(z) = \exp(\rho \cos \theta + i\rho \sin \theta) \\ \quad = \exp(\rho \cos \theta) \cdot \exp(i\rho \sin \theta) \\ \quad = \{\exp(\rho \cos \theta), \rho \sin \theta\} \end{cases} \quad (21)$$

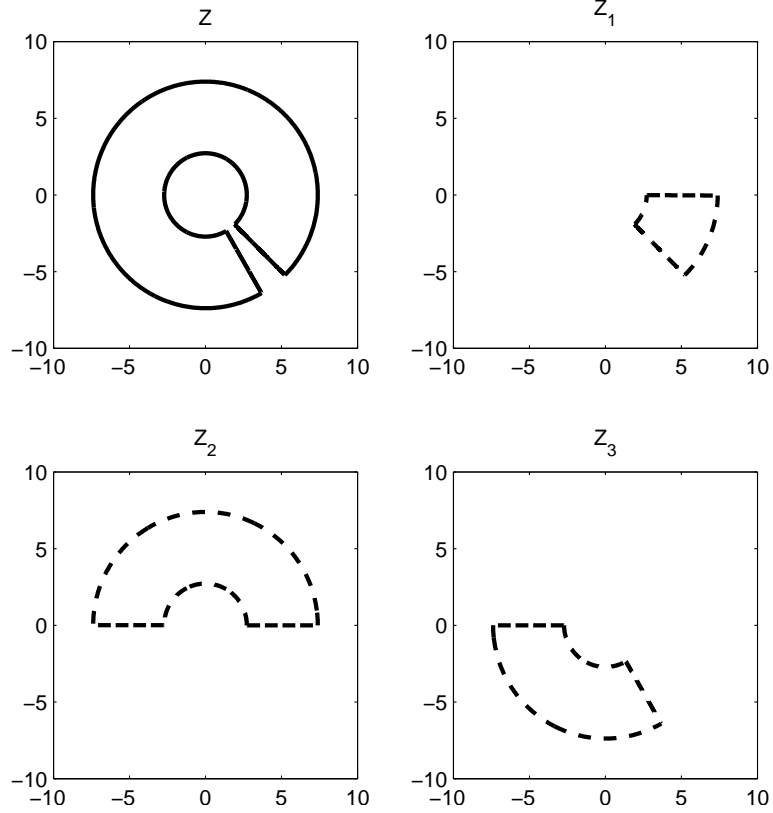


Fig. 4. Sector Z splitted into Z_1 , Z_2 and Z_3 , x-axis is real part and y-axis is imaginary part.

Hence, the natural inclusion function of (21) defined by:

$$\exp(Z) = \{\exp([\rho] \cos([\theta])), [\rho] \sin([\theta])\} \quad (22)$$

gives the exact range of the function $\exp(Z)$. Nevertheless, the bounds of the angle $[\rho] \sin([\theta])$ may not satisfy the condition (6), which means that the angle $[\phi]$ of $\exp(Z)$ should be chosen such that:

$$[\phi] = [\rho] \sin([\theta]) + 2k\pi, \quad i \in \mathbb{Z} \quad (23)$$

where the bounds of $[\phi]$ satisfy (6).

Remark: The hyperbolic functions such as \cosh , \sinh , and \tanh can be easily computed by using the inclusion function $\exp(Z)$ defined in (22).

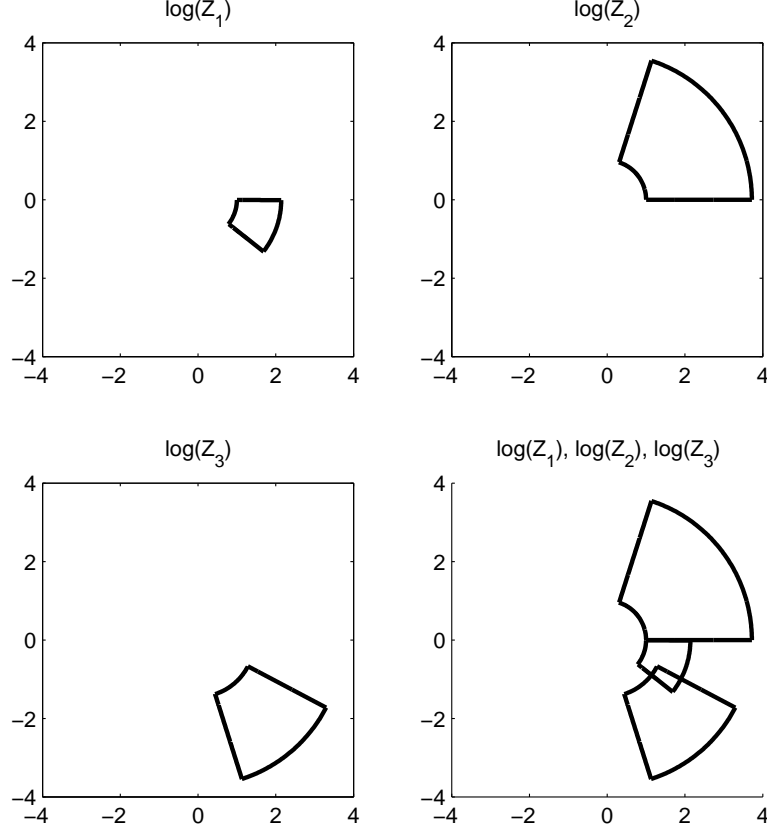


Fig. 5. Logarithm of Z_1 , Z_2 , Z_3 , their union and the convex hull, x-axis is real part and y-axis is imaginary part.

3.4 Enclosure of the range of $\operatorname{acosh}(Z)$

We propose in this section an enclosure of the reciprocal function of $\cosh(Z)$ defined by:

$$\operatorname{acosh}(z) = \log(z + \sqrt{z^2 - 1}) \quad (24)$$

Denote by $t = \{r, \phi\} = z^2 - 1$, then:

$$\sqrt{t} = \begin{cases} t_1 = \{\sqrt{r}, \frac{\phi}{2}\} \\ t_2 = \{\sqrt{r}, \frac{\phi}{2} + \pi\} \end{cases}$$

which means that the equation $y = \log(z + \sqrt{z^2 - 1})$ has two solutions. Hence, the minimal inclusion function of $\operatorname{acosh}(Z)$ is given by:

$$\operatorname{acosh}(Z) = \bigcup(f_1(Z), f_2(Z)) \quad (25)$$

where:

$$\sqrt{t} = \begin{cases} f_1(Z) = \log(Z + T_1) \\ f_2(Z) = \log(Z + T_2) \\ T_1, T_2 : \text{ square roots of } (Z^2 - 1) \end{cases}$$

Note that the $\log(Z + T_i)_{i=1,2}$ could be an union of sectors as described previously.

Remark: For degenerate intervals, we have always $z + \sqrt{z^2 - 1} \neq 0$. This is not the case for non-degenerate intervals because of the wrapping effect. Hence,

$$\text{acosh}(Z) = \{[0, +\infty[, [0, 2\pi]\}, \quad \text{if } 0 \in (Z + \sqrt{Z^2 - 1}).$$

4 Constraint propagation on polar intervals

Consider the constraint satisfaction problem (CSP)

$$\mathcal{H} : (f(\mathbf{z}) = 0, \mathbf{z} \in \mathbb{Z} \in S(\mathbb{C}^n)) \quad (26)$$

where $f : \mathbb{C}^n \rightarrow \mathbb{C}$ and denote by \mathbb{S} the solution set of (26).

Given $Z \in \mathbb{Z}$, an operator \mathcal{C} is called a contractor if:

$$\mathcal{C}(Z) \cap \mathbb{S} \subseteq [Z] \cap \mathbb{S} \quad (27)$$

Hence, a contractor permits to reduce the searching space without performing any bisection.

The computation of $\mathcal{C}(Z) \cap \mathbb{S}$ can be obtained by the extension of the theorem 1 of (Jaulin, 2000) to complex variables. Assume that it is possible to proceed with an explicit inversion of (26), i.e.

$$\forall i \in \{1, \dots, n\}, \exists g^i \mid f(z) = 0 \Leftrightarrow z_i = g^i({}^i z) \quad (28)$$

where ${}^i z = (z_1, \dots, z_{i-1}, z_{i+1}, \dots, z_n)^T$.

Denote by $[g^i]$ an inclusion function for g^i and by Z_i a domain for the variable z_i , then the projection $\pi(\mathbb{S})$ of the solution set \mathbb{S} with respect to the i^{th} axis

satisfies

$$\pi(\mathbb{S}) \subseteq [g^i]([z]) \cap Z_i \quad (29)$$

In several cases, the explicit inversion is not available or given by a very complicated expression; hence, a decomposition of the (CSP) into some primitive constraints is then necessary.

The algorithm used is based on complex interval extension of the local Waltz filtering (Waltz, 1975). In fact, the relationships (26) between the variables can be viewed as a network where the nodes are connected with the constraints. In order to spread the consequences of each node throughout the network, the main idea is to deal with a local group of constraints and nodes and then record the changes in the network. Further deductions will make use of these changes to make further changes. The inconsistent values for the parameter vector are thus removed. If the network exhibits no cycles, then optimal filtering can be achieved by performing only one forward and one backward propagation: this is known as the *forward-backward contractor* (Jaulin et al., 2001).

In this paper, we propose to extend the forward-backward contractor to polar intervals using the arithmetic operations $\{+, -, *, /\}$ and the classical functions i.e. $\{exp, log, cosh, \dots\}$ defined in the previous sections.

Example: Consider the (CSP)

$$\mathcal{H} : \begin{cases} z_3 - z_2 \log(z_1) = 0 \\ z_1 \in \{1, [\frac{2\pi}{3}, \frac{4\pi}{3}]\} \\ z_2 \in \{[1, 3], \frac{\pi}{6}\} \\ z_3 \in \{[2, 10], [\frac{\pi}{2}, \pi]\} \end{cases} \quad (30)$$

The constraint can be decomposed into three *primitive* constraints such that:

$$\begin{aligned} a_1 &= \text{Log}(z_1) \\ a_2 &= z_2 a_1 \\ z_3 - a_2 &= 0 \end{aligned} \quad (31)$$

where the domains for the introduced variables a_i are given by the sector $\{[0, +\infty[, [0, 2\pi]\}$.

The forward propagation is performed by:

$$\begin{aligned}
A_1 &= \text{Log}(Z_1) \cap A_1 \\
A_2 &= Z_2 A_1 \cap A_2 \\
Z_3 &= A_2 \cap Z_3
\end{aligned} \tag{32}$$

where A_i and Z_i are the domains for the variables a_i and z_i . Often the exact evaluation of the *logarithm* function over a polar interval is not a connected set but is a union of disjoint sectors which is characterized via the convex hull as defined in (20). Consequently, the inversion of the primitive constraint *logarithm* would be obtained by computing first the convex hull and then by doing projection. Obviously, it may be useful to perform projection before computing the convex hull. Let us assume $\text{Log}(Z_1) = \bigcup_{i=1,\dots,4} \text{log}(Z_{1i})$, then the first constraint in (32) should be written as

$$A_1 = \text{ConvexHull}(\{\text{log}(Z_{1i}) \cap A_1\}_{i=1,\dots,4}) \tag{33}$$

For the considered example, we obtain:

$$\begin{aligned}
A_1 &= \left\{ \left\{ \frac{2\pi}{3}, \frac{\pi}{2} \right\} \cup \left\{ \frac{2\pi}{3}, \frac{3\pi}{2} \right\} \right\} \cap \{] - \infty, +\infty[, [0, 2\pi] \} \\
&= \left\{ \frac{2\pi}{3}, \frac{\pi}{2} \right\} \cup \left\{ \frac{2\pi}{3}, \frac{3\pi}{2} \right\} \\
A_2 &= \{ [1, 3], \frac{\pi}{6} \} \cdot \left\{ \left\{ \frac{2\pi}{3}, \frac{\pi}{2} \right\} \cup \left\{ \frac{2\pi}{3}, \frac{3\pi}{2} \right\} \right\} \cap \{] - \infty, +\infty[, [0, 2\pi] \} \\
&= \left\{ \left[\frac{2\pi}{3}, 2\pi \right], \frac{2\pi}{3} \right\} \cup \left\{ \left[\frac{2\pi}{3}, 2\pi \right], \frac{5\pi}{3} \right\} \\
Z_3 &= \left\{ \left\{ \left[\frac{2\pi}{3}, 2\pi \right], \frac{2\pi}{3} \right\} \cup \left\{ \left[\frac{2\pi}{3}, 2\pi \right], \frac{5\pi}{3} \right\} \right\} \cap \{ [2, 10], \left[\frac{\pi}{2}, \pi \right] \} \\
&= \left\{ [2, 2\pi], \frac{2\pi}{3} \right\}
\end{aligned}$$

We remark that the domain of the variable z_3 is contracted, the backward propagation phase permits to propagate the changes of Z_3 on the other variables. The backward propagation is given by:

$$\begin{aligned}
A_2 &= Z_3 \cap A_2 \\
A_1 &= A_2 / Z_2 \cap A_1 \\
Z_2 &= A_2 / A_1 \cap Z_2 \\
Z_1 &= \exp(A_1) \cap Z_1
\end{aligned} \tag{34}$$

Then we obtain

$$\begin{aligned}
A_2 &= \{[2, 2\pi], \frac{2\pi}{3}\} \\
A_1 &= \left\{ \{[2, 2\pi], \frac{2\pi}{3}\} / \{[1, 3], \frac{\pi}{6}\} \right\} \cap \left\{ \left\{ \frac{2\pi}{3}, \frac{\pi}{2} \right\} \cup \left\{ \frac{2\pi}{3}, \frac{3\pi}{2} \right\} \right\} \\
&= \left\{ \frac{2\pi}{3}, \frac{\pi}{2} \right\} \\
Z_2 &= \left\{ \{[2, 2\pi], \frac{2\pi}{3}\} / \left\{ \frac{2\pi}{3}, \frac{\pi}{2} \right\} \right\} \cap \left\{ [1, 3], \frac{\pi}{6} \right\} \\
&= \left\{ [1, 3], \frac{\pi}{6} \right\} \\
Z_1 &= \exp\left(\left\{ \frac{2\pi}{3}, \frac{\pi}{2} \right\}\right) \cap \left\{ 1, \left[\frac{2\pi}{3}, \frac{4\pi}{3} \right] \right\}
\end{aligned}$$

Finally we remark that the domains for the variables z_1, z_2 and z_3 are contracted without performing any bisection. In addition the polar representation is suitable when nonlinear function such as *log*, *exp*, . . . and multiplication have to be evaluated.

5 The experimental study

The experimental procedure under analysis hereafter is devoted to the estimation of thermal properties of materials. The thermal diffusivity, denoted by a , and the thermal conductivity λ of a sample are simultaneously measured by using a so-called periodic method which is based on the excitation of the system by multi-harmonic heating signals (Boudenne et al., 2004).

The experimental set-up is shown on figure 6. The sample under study is held in between a metallic rack, with a thermal grease ensuring good thermal exchange between the sample and the metallic rack. The front side of the rack, made of brass, is also fixed to a heating device. The rear side, made of copper, is in contact with air at ambient temperature and high vacuum. Experimental data is given as the following frequency response:

$$H(s) = \frac{T_{rear}(s)}{T_{front}(s)} \quad (35)$$

with $s = j2\pi f$, and the temperature spectra are given by the Fourier transform of the time-history signals. In this paper, we propose to solve the parameter estimation problem in a bounded error context.

5.1 The model

In a periodic mode, the thermal behaviour of each material can be described by a one-dimensional quadrupole (two-port transfer functions). The quadrupole is

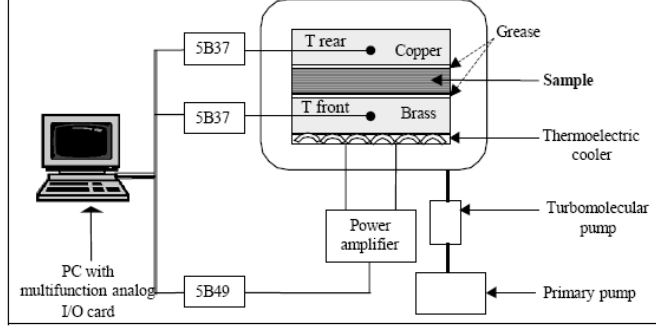


Fig. 6. The experimental set-up

obtained by analytically solving the traditional equations of thermal diffusion. The quadrupole method is well known and extensively used in thermal sciences (Wang et al., 2002).

A "quadrupole" $Z(s)$ is given by:

$$Z(s) = \begin{bmatrix} \cosh(\sqrt{\tau s}) & \frac{R}{\sqrt{\tau s}} \sinh(\sqrt{\tau s}) \\ \frac{\sqrt{\tau s}}{R} \sinh(\sqrt{\tau s}) & \cosh(\sqrt{\tau s}) \end{bmatrix} \quad (36)$$

where: $\tau = \frac{\delta^2}{a}$ is the sample material Fourier time, $R = \frac{\delta}{\lambda}$ is the sample material thermal resistance; δ : sample material thickness, a its diffusivity and λ its conductivity.

Since the model based on the quadrupole theory can be written using the parameters τ and R , the parameter vector to be estimated is chosen as:

$$\mathbf{p}^T = (p_1, p_2)^T = (R, \sqrt{\tau})^T \quad (37)$$

For the particular case of the grease layer, which is assumed without inertia, the relationship uses the resistance only and becomes:

$$Z_{Gre}(s) = \begin{bmatrix} 1 & R \\ 0 & 1 \end{bmatrix} \quad (38)$$

Denote by Z_{Bra} , Z_{Gre} , Z_{Sam} and Z_{Copp} the quadrupole corresponding to re-

spectively Brass, Grease, sample to be characterized, and Copper materials. Hence, the front temperature and flux are given by:

$$\begin{bmatrix} T_{front} \\ \phi_{front} \end{bmatrix} = Z_{Bra}Z_{Gre}Z_{Sam}Z_{Gre}Z_{Copp} \begin{bmatrix} T_{rear} \\ \phi_{rear} \end{bmatrix} \quad (39)$$

And the rear temperature and flux are given by:

$$\begin{bmatrix} T_{rear} \\ \phi_{rear} \end{bmatrix} = Z_{Copp_half} \begin{bmatrix} T_0 \\ \phi_0 \end{bmatrix} \quad (40)$$

where T_0 and ϕ_0 are rear face surface temperature and flux. Now, assume that the coefficient, denoted by h , modelling surface heat exchanges with ambient air, is constant. Hence, the convection phenomenon with ambient air is modelled by:

$$\phi_0(s) = hT_0(s) \quad (41)$$

Finally, by using the equations (36)-(41), we obtain the analytical expression of equation (35).

5.2 The measured data

The signal delivered by the heat source is a sum of five sinusoidal signals; it is given by:

$$u(t) = U_0 + \sum_{i=1}^5 U_i \sin(2\pi f_i t) \quad (42)$$

with $f_i = 2^{i-1}f_1$, $f_1 = 0.781\text{mHz}$, $U_0 = 10$, $U_1 = 1.014$, $U_2 = 1.384$, $U_3 = 1.74$, $U_4 = 2.387$, $U_5 = 3.081$ °C. For each frequency f_i , 30 measurement series j in the same conditions are performed. During each one of these series, the temperatures of the front face $T_{front}^j(t)$ and the rear face $T_{rear}^j(t)$ are provided using thermocouples. After amplification, the signals collected are low-pass filtered ($f_c = 4\text{Hz}$). Finally, the Fourier transform provides a frequency response, H_i^j , for each series:

$$H_i^j(f_i) = \frac{T_{rear}^j(f_i)}{T_{front}^j(f_i)}$$

5.3 Complex interval approximations of actual data

The set of the feasible values of the uncertain data H_i is given by:

$$\mathbb{H}_i = \bigcup_{j=1 \dots 30} H_i^j \quad (43)$$

The experimental data \mathbb{H}_1 for the frequency f_1 are given in figures 3 and 7, where X-axis represents the real part of the transfer function whereas Y-axis represents the imaginary part. As only a finite number of actual experimental data is available, the set \mathbb{H}_i is approximated by a complex interval domain. The simplest complex interval characterization is the rectangular one, where the complex-shaped set \mathbb{H}_i is approximated by an axis-aligned rectangle. The set \mathbb{H}_1 and the smallest rectangle containing it are plotted in figure 7.

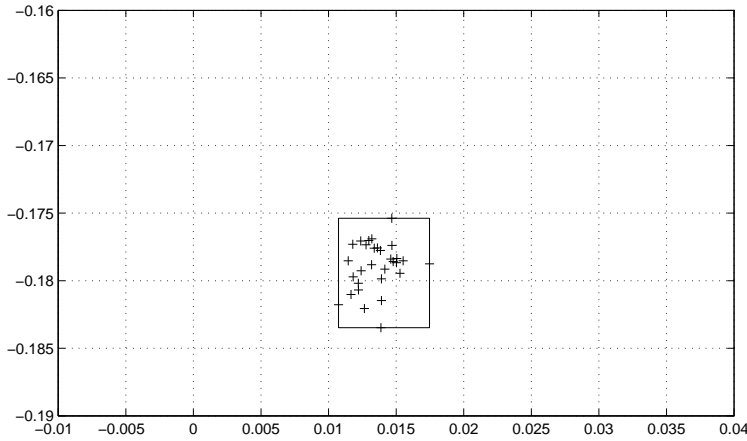


Fig. 7. The smallest rectangle approximating the measured data \mathbb{H}_1

In addition, the set \mathbb{H}_i can also be characterized by a sector. In such a case, the polar intervals presented in this paper are used. The set \mathbb{H}_1 and the smallest sector containing it are plotted in figure 8.

5.4 Polar versus rectangular form for the inclusion test

The thermal parameters are estimated by using the algorithm SIVIA. Hence, we have only to define an inclusion test, i.e. a test which permits to verify if a box $[\mathbf{p}]$ is feasible, and a contractor. Here we use the forward-backward contractor as defined in section 4.

To prove that a box $[\mathbf{p}]$ is feasible, one should verify that:

$$[H](f_i, [\mathbf{p}]) \subseteq [\mathbb{H}_i], \quad \forall i \in \{1, \dots, N\} \quad (44)$$

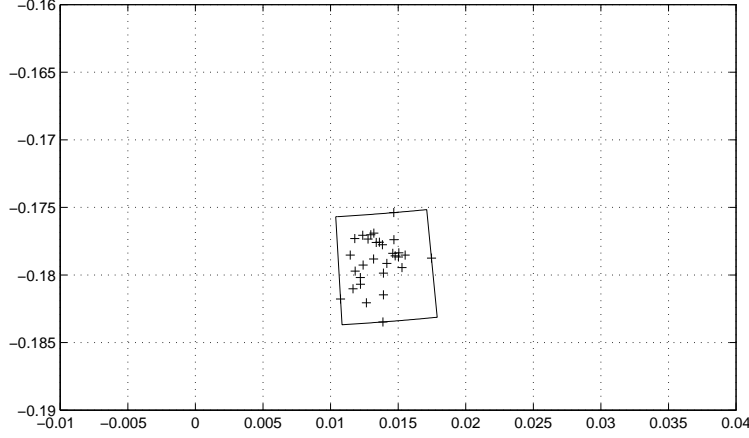


Fig. 8. The smallest sector approximating the measured data \mathbb{H}_1

To prove that a box $[\mathbf{p}]$ is unfeasible, one should prove that:

$$\exists i \in \{1, \dots, N\}, \quad [H](f_i, [\mathbf{p}]) \cap [\mathbb{H}_i] = \emptyset \quad (45)$$

where $[H]$ is an inclusion function for H and $[\mathbb{H}_i]$ is the smallest complex interval containing the set \mathbb{H}_i . In the following, we denote respectively by $[\mathbb{H}_i^r]$ and $[\mathbb{H}_i^p]$ the rectangle and the sector containing \mathbb{H}_i . Similarly, we denote by $[H^r]$ and $[H^p]$ the inclusion functions respectively based on the rectangular and the polar arithmetics.

Example: Assume that $[\mathbf{p}] = [0.0298124, 0.0300508] \times [14.5938, 14.7071]$. The evaluation of $[H^r]$ and $[H^p]$ for the frequencies: $f_1 = 0.781mHz$, $f_2 = 1.562mHz$, $f_3 = 3.125mHz$, $f_4 = 6.25mHz$ and $f_5 = 12.5mHz$ are given by the tables 1 and 2.

| Frequency (mHz) | $[H^p]$ | Data |
|-----------------|--|---|
| 0.781 | $\{[0.1776, 0.1821], [4.7717, 4.7852]\}$ | $\{[0.176, 0.1841], [4.7713, 4.8098]\}$ |
| 1.562 | $\{[0.0891, 0.0915], [4.4858, 4.4988]\}$ | $\{[0.0887, 0.092], [4.4728, 4.5372]\}$ |
| 3.125 | $\{[0.0420, 0.0433], [4.1004, 4.1144]\}$ | $\{[0.0407, 0.04391], [4.0712, 4.1384]\}$ |
| 6.25 | $\{[0.0171, 0.0178], [3.4968, 3.5153]\}$ | $\{[0.0155, 0.02], [3.42, 3.5814]\}$ |
| 12.5 | $\{[0.0053, 0.0056], [2.6119, 2.6364]\}$ | $([0.0009, 0.0084], [3.1813, 9.421])$ |

Table 1

Evaluations of the polar inclusion function and real data

| Frequency (mHz) | $[H^p]$ | Data |
|-----------------|--|--|
| 0.781 | $[0.0085, 0.0154] + i[-0.1915, -0.1681]$ | $[0.0107, 0.0175] + i[-0.1834, -0.1754]$ |
| 1.562 | $[-0.0224, -0.0173] + i[-0.0947, -0.082]$ | $[-0.0216, -0.0158] + i[-0.0898, -0.087]$ |
| 3.125 | $[-0.0264, -0.0222] + i[-0.0379, -0.0325]$ | $[-0.0253, -0.0226] + i[-0.0364, -0.0335]$ |
| 6.25 | $[-0.018, -0.0148] + i[-0.0071, -0.0054]$ | $[-0.0189, -0.0144] + i[-0.0077, -0.0045]$ |
| 12.5 | $[-0.0053, -0.0042] + i[0.0023, 0.0032]$ | $[-0.0073, 0.0004] + i[-0.0025, 0.007]$ |

Table 2

Evaluations of the rectangular inclusion function and real data

The evaluations of $[H^p]$ and $[H^r]$ for f_1 are plotted on figure 9 and figure 10. Hence, we remark that $[H^p](f_1, [\mathbf{p}])$ is contained in the smallest sector including the measured data. Similarly, we can easily verify such a property for the other frequencies. Therefore, we can conclude that when using polar complex intervals the inclusion test is satisfied for the five frequencies, i.e.

$\forall \mathbf{p} \in [\mathbf{p}] = [0.0298124, 0.0300508] \times [14.5938, 14.7071], H_i(\mathbf{p}) \in \mathbb{H}_i$. Hence, the box $[\mathbf{p}] = [0.0298124, 0.0300508] \times [14.5938, 14.7071]$ is deemed feasible.

On the contrary, the results are different when rectangular complex intervals are used. Due to the pessimism induced by the rectangular form, the box $[\mathbf{p}] = [0.0298124, 0.0300508] \times [14.5938, 14.7071]$ is now deemed ambiguous and must be splitted to achieve a conclusion (see figure 10). Obviously, the polar inclusion function is more suitable for the model under study.

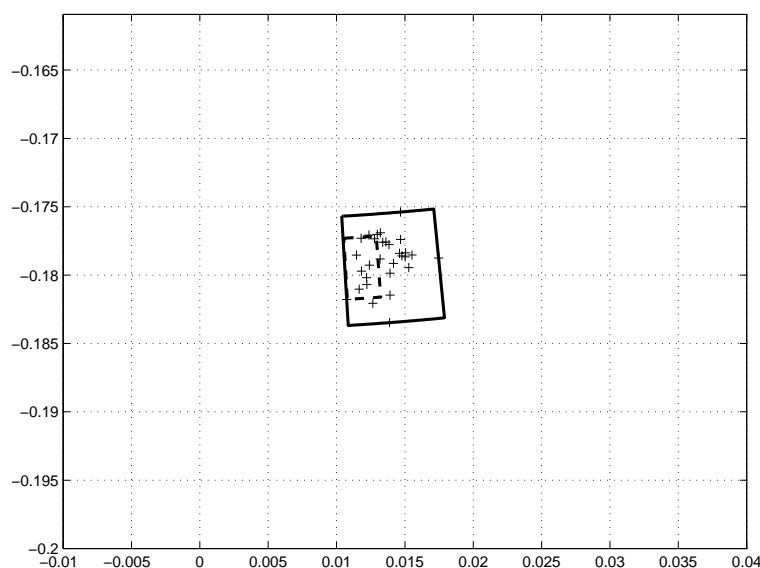


Fig. 9. Evaluation of $[H^p](f_1, [\mathbf{p}])$. Dashed line: evaluation of $[H^p]$, sold line: the smallest sector containing the measured data

5.5 Polar versus rectangular form for set inversion

Error bounds on the experimental transfer function are calculated prior to the identification from measurements repeated 30 times. For the sample under study, prior searching space for the parameters are:

$$\begin{cases} p_1 \in [10^{-4}, 5] \\ p_2 \in [1, 1000] \end{cases} \quad (46)$$

First, we will compare SIVIA results when no contractor is used and for the two inclusion tests, i.e. with a natural inclusion function based on the polar

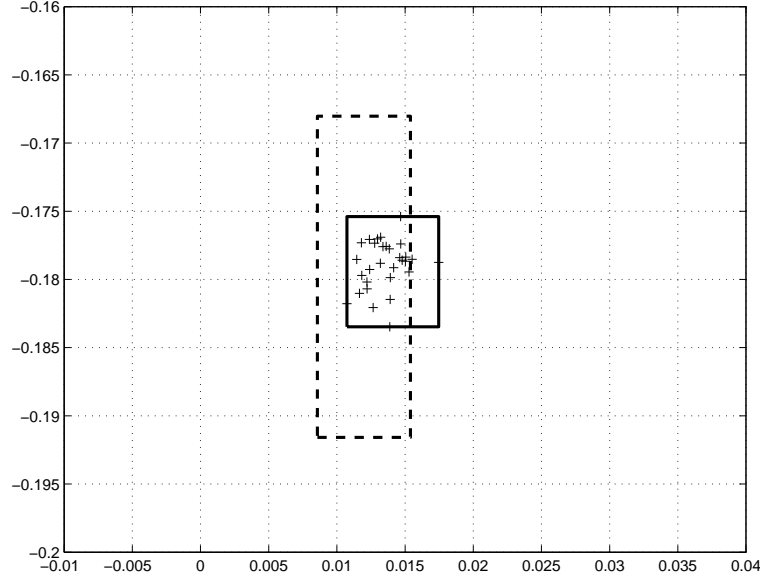


Fig. 10. Evaluation of $[H^r](f_1, [\mathbf{p}])$. Dashed line: evaluation of $[H^r]$, sold line: the smallest rectangle containing the measured data

complex interval representation and the one based on rectangular complex intervals.

5.5.1 Polar form

With polar form, SIVIA generates in 20s the set of the boxes plotted on figure 11. The projection of the outer approximation gives the feasible domain of the parameter vector. Hence, we obtain:

$$p_1 \in [0.029097, 0.030736] \text{ and } p_2 \in [14.254, 15.1036]$$

Thus, the uncertainty domains for the thermal parameters are:

$$a \in [0.10959, 0.123045] \times 10^{-6} \text{u.SI}$$

$$\lambda \in [0.16267, 0.17183] \text{u.SI}$$

5.5.2 Rectangular form

Now, SIVIA without a contractor but with a natural inclusion function based on the rectangular complex interval representation generates in 60s the set of the boxes plotted on figure 12. The projection of the outer approximation gives the feasible domain of the parameter vector. Hence, we obtain:

$$p_1 \in [0.028993, 0.030915] \text{ and } p_2 \in [14.0274, 15.0752]$$

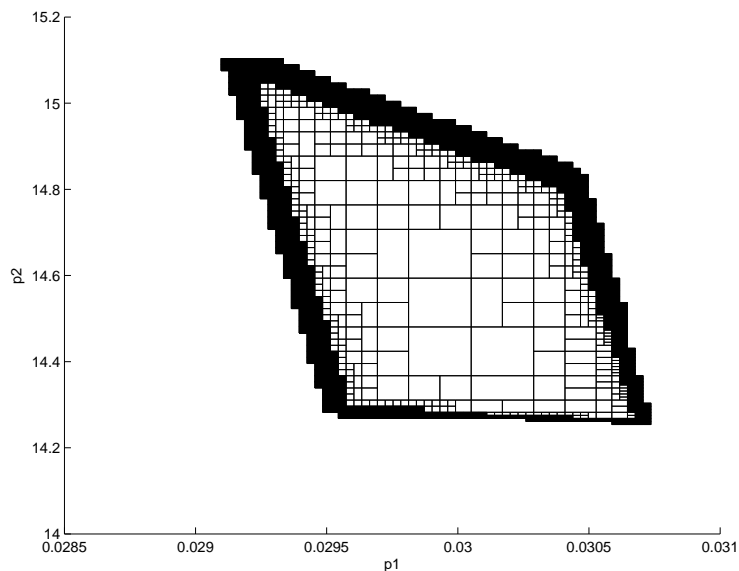


Fig. 11. Inner and outer approximations generated by SIVIA with polar representation

Thus, the domains for the thermal parameters are:

$$a \in [0.11, 0.12705] \times 10^{-6} \text{u.SI}$$

$$\lambda \in [0.16173, 0.17245] \text{u.SI}$$

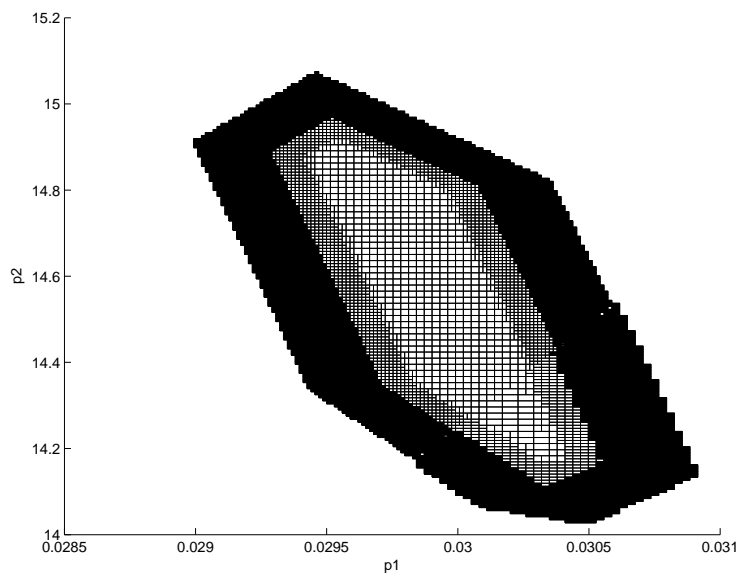


Fig. 12. Inner and outer approximations generated by SIVIA with rectangular representation

As given in the table 5.5.2, the computing time is longer when the rectangular representation is used. Indeed, as already stated earlier, the latter introduces

some pessimism and the parameter vector need be further splitted.

| | Polar form | Rectangular form |
|----------------|------------|------------------|
| Computing time | 20 | 60 |

Table 3

Computing time in seconds for polar and rectangular representations without contraction

5.5.3 Comparison of the splitting number for the polar and rectangular representations

To compare the polar and the rectangular representations, The number of bisections needed for the algorithm SIVIA with an inclusion functions respectively based on the rectangular and the polar representations is given in the table 3. We note that the polar form permits to reduce the number of bisections of the parameter vector domain; hence, the computing time is less important. In fact, the model is described by a strongly non-linear function. In such a case, the inclusion function based on the rectangular form is more pessimistic. In the other hand, we remark that the parameter vector is less bisected when a contractor is used.

| Representation | Polar | Rectangular | Polar and Rectangular |
|---------------------|-------|-------------|-----------------------|
| Without contraction | 4103 | 22139 | 7443 |
| With contraction | 3285 | 17229 | 6957 |

Table 4

Bisection number

5.6 Combination of polar and rectangular representations for set inversion

As indicated in section 5.2, the domains of the measured data are not given by complex intervals; hence, a pessimism is introduced. To reduce the effect of this pessimism on the estimated parameters, we propose to use simultaneously the rectangular and the polar representations. SIVIA generates, in 116 s, the set of the boxes plotted on figure 13. In this case, the feasible set is computed by the intersection of the feasible sets obtained using the polar and the rectangular representations. The projection of the outer approximation gives the uncertainty on the parameter vector. Hence, we obtain:

$$p_1 \in [0.028859, 0.031005] \text{ and } p_2 \in [14.1973, 15.1602]$$

Thus, the uncertainty domains for the thermal parameters are:

$$a \in [0.10877, 0.12403] \times 10^{-6}$$

$$\lambda \in [0.16126, 0.17325]$$

We remark that by using both the rectangular and polar representations, the uncertainties on the estimated parameters are reduced.

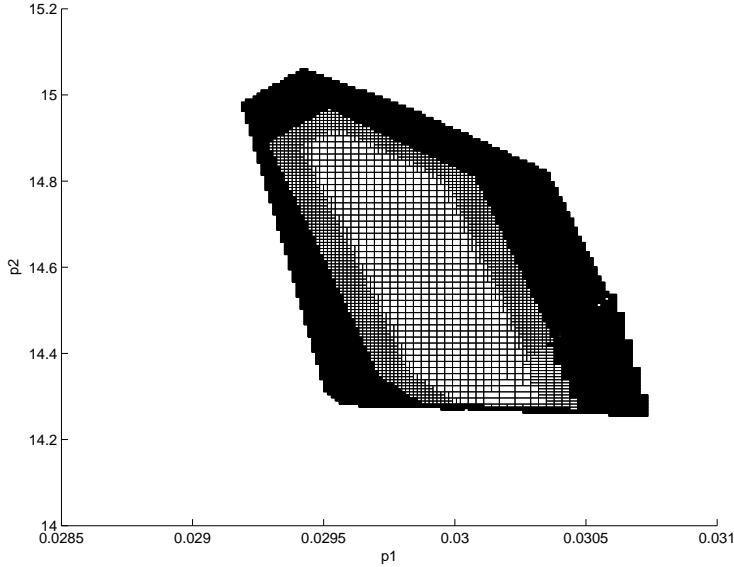


Fig. 13. Inner and outer approximations generated by SIVIA with rectangular representation

6 Conclusion

This paper addresses bounded error parameter identification for complex-valued non-linear models. The set inversion algorithm SIVIA is used to compute the set of all the parameter vectors such as the model output is consistent with the measured data and the error bounds. SIVIA is based on an inclusion test which needs the evaluation of the complex-valued model over complex intervals. In this paper, the main functions, such as \ln , \exp , acosh , are extended to polar intervals. In the other hand, two complex interval representations are compared: polar and rectangular forms. Finally, we showed that using simultaneously polar and rectangular representations permits to reduce the pessimism on the estimated parameters.

In order to reduce the pessimism and so the computing time, we propose in a future work to use other inclusion functions based on Taylor forms. In such a context, the derivatives of the complex-valued functions are needed. To compute these derivatives, automatic differentiation on polar intervals should be investigated.

References

- Milanese, M., J.P. Norton, H. Piet-Lahanier and E. Walter, *Bounding approaches to system identification*, New York: Plenum (1996).
- Durieu, C., E. Walter, and B Polyak, Multi-Input Multi-Output Ellipsoidal State Bounding, *J. Opt. Theory Applications*, 111(2) (2001) 273-303.
- Maksarov, D.G. and J.P. Norton, Computationally efficient algorithms for state estimation with ellipsoidal approximation, *International Journal of Adaptive Control and Signal Processing*, 16(6) (2002) 411-434.
- Jaulin, L. and E. Walter, Set inversion via interval analysis for non linear bounded-error estimation, *Automatica*, 29(4) (1993) 1053-1064.
- Jaulin, L., M. Kieffer, O. Didrit and E. Walter, *Applied Interval Analysis*, London: Springer (2001).
- L. Jaulin, Interval constraint propagation with application to bounded-error estimation, *Automatica*, 36 (2000) 1547-1552.
- Alefeld G. and Herzberger J., *Introduction to interval computations*, Academic Press, New York (1983).
- Petkovic M. S. and Petkovic L. D., *Complex interval arithmetic and its applications*, Wiley-VCH, Berlin (1998).
- Henrici P., *Circular arithmetic and the determination of polynomial zeros*, Springer Lecture Notes, 228 (1971) 86-92.
- Klatte R. and Ullrich C., Complex sector arithmetic, *Computing*, 24(2-3) (1980) 139-148.
- Rokne J. and Lancaster P., Complex interval arithmetic, *ACM*, 14 (1971) 111-112.
- Candau Y., Raissi T., Ramdani N. and Ibos L., Complex interval arithmetic using polar form, *Reliable Computing*, 12(1) (2006) 1-20.
- Farouki R. T., Pottmann H., Exact Minkowski Products of N Complex Disks, *Reliable Computing*, 8 (2002) 43-66.
- Hansen E., *Global optimisation using interval analysis*, Marcel Dekker, New York (1992).
- Havriliak Jr S., Havriliak S.J., *Dielectric and Mechanical Relaxation in Materials*, Hanser, Munich (1997).
- Kearfott R. B., *Rigorous global search: continuous problems*, Kluwer Academic Publishers, Dordrecht, Netherlands (1996).
- T. Sunaga, Theory of interval algebra and its application to numerical analysis, In: *RAAG Memoirs, Ggujustu Bunken Fukuy-kai*. Tokyo, vol.2 (1958) 29-46.
- Moore R. E., *Interval analysis*, Prentice Hall, Englewood Clis, NJ (1966).
- Neumaier A., *Interval methods for systems of equations*. Cambridge University Press, Cambridge, 1990.
- Nickel K., Arithmetic of complex sets, *Computing*, 24 (1980) 97-105.
- D. L. Waltz, Generating semantic descriptions from drawings of scenes with shadows. In P. H. Winston, *The psychology of computer vision*, 1991, New York: McGraw-Hill, 1975.
- Boudenne, A., L. Ibos, E. Géhin and Y. Candau, A simultaneous character-

ization of thermal conductivity and diffusivity of polymer materials by a periodic method, *J. Phys. D: Appl. Phys.*, 37 (2004) 132-139.

Wang H., Degiovanni A. and Moyne C., Periodic thermal contact : a quadrupole model and an experiment, *Int. J. Therm. Sci.*, 41 (2002) 125-135.